The EMBO Journal (2011) 30, 2465–2476 | © 2011 European Molecular Biology Organization | All Rights Reserved 0261-4189/11
www.embojournal.org

THE EMBO JOURNAL

Daxx mediates activation-induced cell death in microglia by triggering MST1 signalling

Hee Jae Yun[1], Je-Hyun Yoon[1], Jae Keun Lee[1], Kyung-Tae Noh[1], Kyoung-Wan Yoon[1], Sang Phil Oh[2], Hyun Jung Oh[2], Ji Soo Chae[1], Sang Gil Hwang[1], Eun Hee Kim[3], Gerd G Maul[4], Dae-Sik Lim[2] and Eui-Ju Choi[1,5,*]

[1]School of Life Sciences and Biotechnology, Korea University, Seoul, Korea, [2]Department of Biological Sciences, Biomedical Research Center, Korea Advanced Institute of Science and Technology, Daejeon, Korea, [3]School of Bioscience and Biotechnology, Chungnam National University, Daejeon, Korea, [4]The Wistar Institute, Philadelphia, PA, USA and [5]School of Pharmacy, Korea University, Yeongi, Chungnam, Korea

Microglia, the resident macrophages of the mammalian central nervous system, migrate to sites of tissue damage or infection and become activated. Although the persistent secretion of inflammatory mediators by the activated cells contributes to the pathogenesis of various neurological disorders, most activated microglia eventually undergo apoptosis through the process of activation-induced cell death (AICD). The molecular mechanism of AICD, however, has remained unclear. Here, we show that Daxx and mammalian Ste20-like kinase-1 (MST1) mediate apoptosis elicited by interferon-γ (IFN-γ) in microglia. IFN-γ upregulated the expression of Daxx, which in turn mediated the homodimerization, activation, and nuclear translocation of MST1 and apoptosis in microglial cells. Depletion of Daxx or MST1 by RNA interference also attenuated IFN-γ-induced cell death in primary rat microglia. Furthermore, the extent of IFN-γ-induced death of microglia in the brain of MST1-null mice was significantly reduced compared with that apparent in wild-type mice. Our results thus highlight new functions of Daxx and MST1 that they are the key mediators of microglial cell death initiated by the proinflammatory cytokine IFN-γ.

The EMBO Journal (2011) **30,** 2465–2476. doi:10.1038/emboj.2011.152; Published online 13 May 2011
Subject Categories: signal transduction
Keywords: cell death; Daxx; interferon-γ; microglia; MST1

Introduction

Microglia are the resident immune cells of the central nervous system. In the resting state, these cells have an immunosurveillance role (Liu and Hong, 2003). In response to infection or brain injury, however, they migrate to the affected region of the central nervous system, where they proliferate and become activated (Streit *et al*, 1999). Activated microglia eventually undergo apoptosis by a process known as activation-induced cell death (AICD) (Kennedy *et al*, 1972; Takeuchi *et al*, 2006; Mayo *et al*, 2008). Although the precise mechanism underlying microglial activation is not fully understood, cytokines such as interferon (IFN)-γ secreted by local inflammatory cells mediate the activation process (Neumann, 2001; Hanisch and Kettenmann, 2007; Pocock and Kettenmann, 2007). Activated microglia secrete neurotrophic factors, thereby promoting the survival of neurons, but they also secrete cytotoxic mediators such as nitric oxide (NO) and cytokines such as TNF-α and IL-1β that induce inflammation and neurotoxicity (Streit *et al*, 1999). Indeed, activated microglia have been shown to be active participants in the pathogenesis of neurodegenerative disorders (Block and Hong, 2005; Block *et al*, 2007; Rogers *et al*, 2007). It is therefore important that the population of activated microglia be strictly regulated, with removal of the activated cells by AICD being thought to be an efficient mechanism for the protection of neurons against their deleterious effects. Cytotoxic factors such as NO and proinflammatory cytokines released from activated microglia have been shown to mediate AICD through the regulation of apoptotic proteins including caspases and Bcl-2 family proteins (Lee *et al*, 2001a; Liu *et al*, 2001; Takeuchi *et al*, 2006; Mayo and Stein, 2007). The molecular mechanism of AICD in microglia, however, remains to be elucidated completely.

Mammalian STE20-like kinase-1 (MST1) is a serine–threonine kinase that belongs to the family of protein kinases related to yeast Ste20 (Creasy *et al*, 1996; Dan *et al*, 2001). MST1 is homologous to the Drosophila Hippo kinase and it is a key component of the Hippo signalling pathway. Most of the components of the Hippo pathway were identified through genetic screens for Drosophila with defects in organ size (Justice *et al*, 1995; Xu *et al*, 1995). The Hippo/MST kinase, when associated with scaffold protein Salvador (WW45 in mammals), phoshorylates and activates Lats/Warts kinase, which in turn phosphoryates the transcription coregulator Yorkie in Drosophila and YAP in mammals (Chan *et al*, 2005; Dong *et al*, 2007; Zhao *et al*, 2007; Hao *et al*, 2008). Phosphorylated Yorkie and YAP are exported from the nucleus and sequestered in the cytoplasm in 14-3-3-dependent and -independent manners (Dong *et al*, 2007; Zhao *et al*, 2007; Oh and Irvine, 2009). Yorkie/YAP upregulates transcription of a number of genes associated with cell proliferation and survival (Yagi *et al*, 1999; Strano *et al*, 2001; Huang *et al*, 2005). Thus, the Hippo pathway inhibits cell proliferation and promotes apoptosis by phosphorylating and inhibiting Yorkie and YAP (Huang *et al*, 2005; Zhao *et al*, 2007). The overall operation of the Hippo pathway is well conserved among mammals and Drosophila. Nevertheless, the regulatory mechanism of MST1 appears to be more complicated than expected from genetic analysis of the Drosophila Hippo pathway.

*Corresponding author. School of Life Sciences and Biotechnology, Korea University, Anam-dong, Sungbuk-ku, Seoul 136-701, Korea.
Tel.: +82 23 290 3446; Fax: +82 23 290 4741;
E-mail: ejchoi@korea.ac.kr

Received: 4 September 2010; revised: 18 April 2011; published online: 13 May 2011

MST1 contains a catalytic domain in the amino-terminal region, an autoinhibitory domain in the central region, and a coiled-coil regulatory SARAH domain in the carboxy-terminal region (Creasy *et al*, 1996; Scheel and Hofmann, 2003). The SARAH domain of MST1 mediates homodimerization as well as heterodimerization with other SARAH-domain-containing proteins such as WW45 and Rassf proteins (Creasy *et al*, 1996; Scheel and Hofmann, 2003). MST1 is expressed ubiquitously and regulates a variety of cellular processes including proliferation, apoptosis, stress responses, morphogenesis, and senescence (de Souza and Lindsay, 2004; Lehtinen *et al*, 2006). In particular, MST1 has been implicated in apoptosis following chromatin condensation and DNA fragmentation as a result of its phosphorylation of histone H2B or other substrate proteins (Cheung *et al*, 2003; Lehtinen *et al*, 2006; Praskova *et al*, 2008; Vichalkovski *et al*, 2008).

To gain insights into the biological functions of MST1, we have investigated the possible role of MST1 in the apoptosis of microglia induced by IFN-γ. We now show that MST1 mediate apoptosis elicited by IFN-γ in microglia. IFN-γ induces expression of Daxx, which in turn mediates homodimerization and activation of MST1 and apoptosis in microglial cells. Moreover, IFN-γ-induced microglial death in the brain was reduced in MST1-null mice, compared with that apparent in wild-type mice. Our results thus suggest that Daxx and MST1 are the critical mediators of microglial cell death initiated by the proinflammatory cytokine IFN-γ.

Results and discussion

MST1 contributes to IFN-γ-induced apoptosis in microglia

Exposure of primary rat microglia to IFN-γ induced the phosphorylation of histone H2B on Ser^{14} in the nucleus together with the formation of apoptotic chromatin bodies (Figure 1A). Given that MST1 mediates the phosphorylation of histone H2B on Ser^{14}, which promotes chromatin condensation associated with apoptosis (Cheung *et al*, 2003), we investigated the possibility that MST1 might contribute to IFN-γ-induced apoptosis in microglial cells. We transfected primary rat microglia with siRNA oligonucleotides specific for MST1 or GFP control mRNA. IFN-γ induced a marked increase in the incidence of apoptosis in microglial cells transfected with control siRNA, but it had no such effect in the cells transfected with MST1 siRNA (Figure 1B). Depletion of MST1 by RNA interference (RNAi) also prevented the IFN-γ-induced phosphorylation of histone H2B on Ser^{14}, suggesting that IFN-γ promoted the stimulation of MST1 activity for phosphorylating histone H2B (Figure 1C). These results thus implicated MST1 as a key mediator of IFN-γ-induced apoptosis in microglia.

Daxx mediates IFN-γ-induced MST1 activation in microglia

To clarify the mechanism by which IFN-γ regulates MST1, we searched for MST1-binding proteins with the use of the yeast two-hybrid assay and a HeLa cell cDNA library. We identified

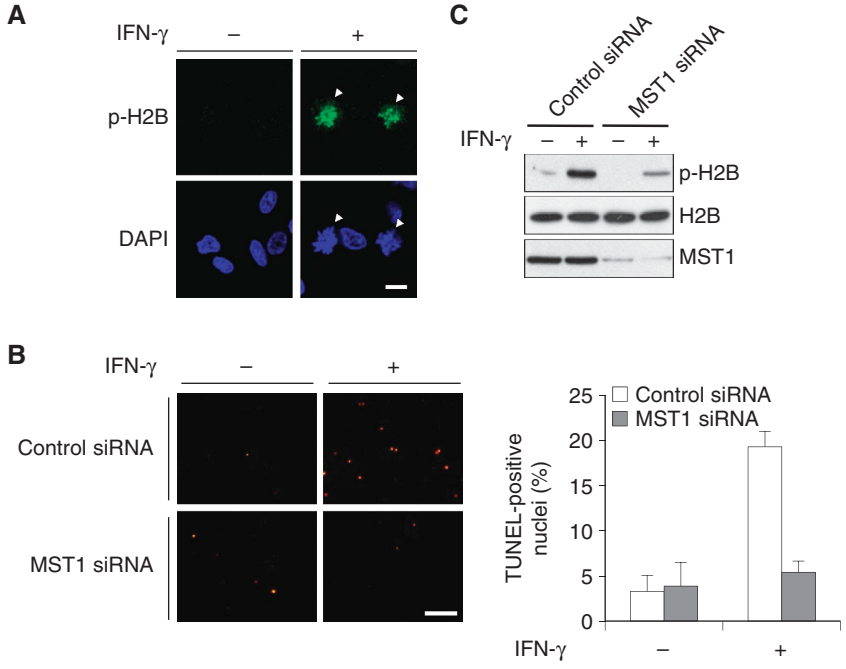

Figure 1 Depletion of MST1 by RNA interference downregulates IFN-γ-induced apoptosis in primary rat microglia. (**A**) Primary rat microglial cells were incubated for 48 h in the absence or presence of IFN-γ (100 U/ml), were then fixed and stained with DAPI. DAPI-stained cells were subjected to immunostaining with antibodies to Ser^{14}-phosphorylated histone H2B and analysed by fluorescence microscopy. Arrowheads indicate cells with condensed nuclei. Scale bars, 10 μm. (**B**) Primary rat microglia were transfected for 24 h with siRNA oligonucleotides targeting GFP (control) or MST1 mRNA and were then incubated for 48 h in the absence or presence of IFN-γ (100 U/ml). Apoptosis was analysed with TUNEL method. Data in the left panel are representative of three independent experiments. Data in the right panel are the mean of triplicate determinations ± s.d. Scale bar, 100 μm. (**C**) Primary rat microglia transfected with GFP or MST1 siRNA oligonucleotides were incubated in the absence or presence of IFN-γ (100 U/ml) for 16 h. Cell lysates were subjected to immunoblot analysis with antibodies to Ser^{14}-phosphorylated histone H2B (p-H2B), to histone H2B, or to MST1.

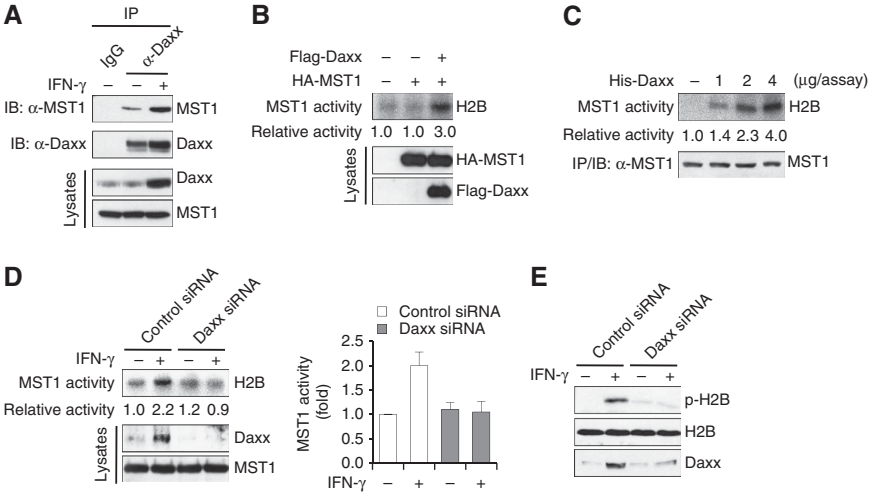

Figure 2 Daxx mediates IFN-γ-induced MST1 activation in microglial cells. (**A**) BV-2 cells were left untreated or treated with IFN-γ (100 U/ml) for 16 h. Cell lysates were subjected to immunoprecipitation (IP) with either goat preimmune IgG (IgG) or anti-Daxx antibody (α-Daxx), and the resulting precipitates were subjected to immunoblot analysis with anti-MST1 antibody. Cell lysates were also immunoblotted with antibodies to Daxx or to MST1. (**B**) 293T cells were transfected for 48 h with expression vectors for HA-MST1 and Flag-Daxx. Cell lysates were subjected to immunoprecipitation with anti-HA antibody, and the resulting precipitates were assayed for MST1 activity by immune complex kinase assay. (**C**) *In vitro* effect of Daxx on MST1 activity. 293T cell lysates were subjected to immunoprecipitation with anti-MST1 antibody. The MST1 immunoprecipitates were incubated at 30°C for 30 min in 20 μl of the kinase reaction buffer in the absence or presence of hexahistidine-tagged Daxx (His-Daxx). The precipitates were washed twice with PBS, and then assayed for the kinase activity with histone H2B as substrate. The equal amount of the immunoprecipitates was also immunoblotted with MST1 antibody. (**D**) (Left) Primary rat microglia transfected with GFP or Daxx siRNA oligonucleotides were incubated in the absence or presence of IFN-γ (100 U/ml) for 16 h. Cell lysates were subjected to immunoprecipitation with anti-MST1 antibody and the resulting precipitates were assayed for MST1 activity by immune complex kinase assay. Cell lysates were also examined directly by immunoblot analysis with antibodies to Daxx and MST1. (Right) MST1 activity (the intensity of the bands corresponding to histone H2B phosphorylation) was quantified by densitometry. Data are mean values ± s.d. from two independent experiments. (**E**) Primary rat microglia transfected with GFP or Daxx siRNA oligonucleotides were left untreated or treated with IFN-γ (100 U/ml) for 16 h, and then lysed. Cell lysates were subjected to immunoblot analysis with antibodies to Ser^{14}-phosphorylated histone H2B (p-H2B), to histone H2B, or to Daxx.

several proteins including WW45 and Rassf1, both of which are known as MST-binding proteins (Khokhlatchev *et al*, 2002; Scheel and Hofmann, 2003; Callus *et al*, 2006), as well as death-associated protein 6 (Daxx). Among the identified proteins, we focused on Daxx because IFN-γ enhanced cellular levels of Daxx in primary rat microglia (Figure 2D) and microglial BV-2 cells (Figure 2A). Furthermore, IFN-γ promoted a physical interaction between Daxx and MST1 in the cells (Figure 2A). IFN-γ also increased MST1 activity in BV-2 cells, with this effect being maximal at 16 h after the onset of exposure to IFN-γ, coincident with the maximal increase in Daxx abundance (Supplementary Figure S1). The IFN-γ-induced increases in both Daxx abundance and MST1 activity in the cells were abolished by AG490, an inhibitor of Janus kinase-2 (Meydan *et al*, 1996), suggesting an involvement of the Janus kinase-2 pathway in IFN-γ-induced Daxx expression (Supplementary Figure S2). Taken together, these observations suggested the possibility that Daxx might mediate IFN-γ-induced MST1 activation in microglial cells.

To examine whether Daxx affects MST1 activity, we transfected 293T cells with plasmids encoding HA-MST1 and Flag-Daxx. Ectopic Daxx increased the kinase activity of MST1 in the transfected cells (Figure 2B). Daxx also increased MST1 activity *in vitro* (Figure 2C), suggesting that Daxx directly activates MST1. It is also noteworthy that MST1 did not phosphorylate Daxx *in vitro* (Supplementary Figure S3). To examine the potential role of Daxx in IFN-γ-induced MST1 activation in microglia, we transfected primary rat microglial cells with GFP (control) or Daxx siRNA oligonucleotides. Immunoblot analysis revealed that IFN-γ treatment increased the abundance of Daxx in the cells transfected with control siRNA, and this effect was abolished in Daxx siRNA-transfected cells (Figure 2D). Concomitantly, IFN-γ increased MST1 activity in control siRNA-transfected cells, and depletion of Daxx by RNAi prevented this effect of IFN-γ. Similar results were observed in separate experiments using BV-2 cells expressing Daxx siRNA (Supplementary Figure S4). The RNAi-mediated depletion of Daxx also abolished the phosphorylation of histone H2B on Ser^{14} in primary rat microglia (Figure 2E). Together, these results suggested that IFN-γ upregulates the expression of Daxx and that Daxx in turn mediates the activation of MST1 in microglial cells.

Daxx physically associates with MST1, thereby promoting the homodimerization of MST1

We next examined which domains of Daxx and MST1 are responsible for the interaction between the two proteins. Ectopically expressed Daxx interacted with MST1 and MST1 (421–487), but not with MST1 (1–420), in 293T cells (Figure 3A). Consistent with these data, *in vitro* binding analysis revealed that Daxx bound to MST1 and MST1 (421–487), but not to MST1 (1–420) (Figure 3B). Furthermore, Daxx induced the activation of MST1 but not that of MST1 (1–420) (Figure 3C). Reciprocal co-immunoprecipitation analysis showed that MST1 bound to Daxx (1–500) and Daxx (1–267), but not to Daxx (268–570) (Figure 3D) or Daxx (498–740) (Supplementary Figure S5). Consistent with these

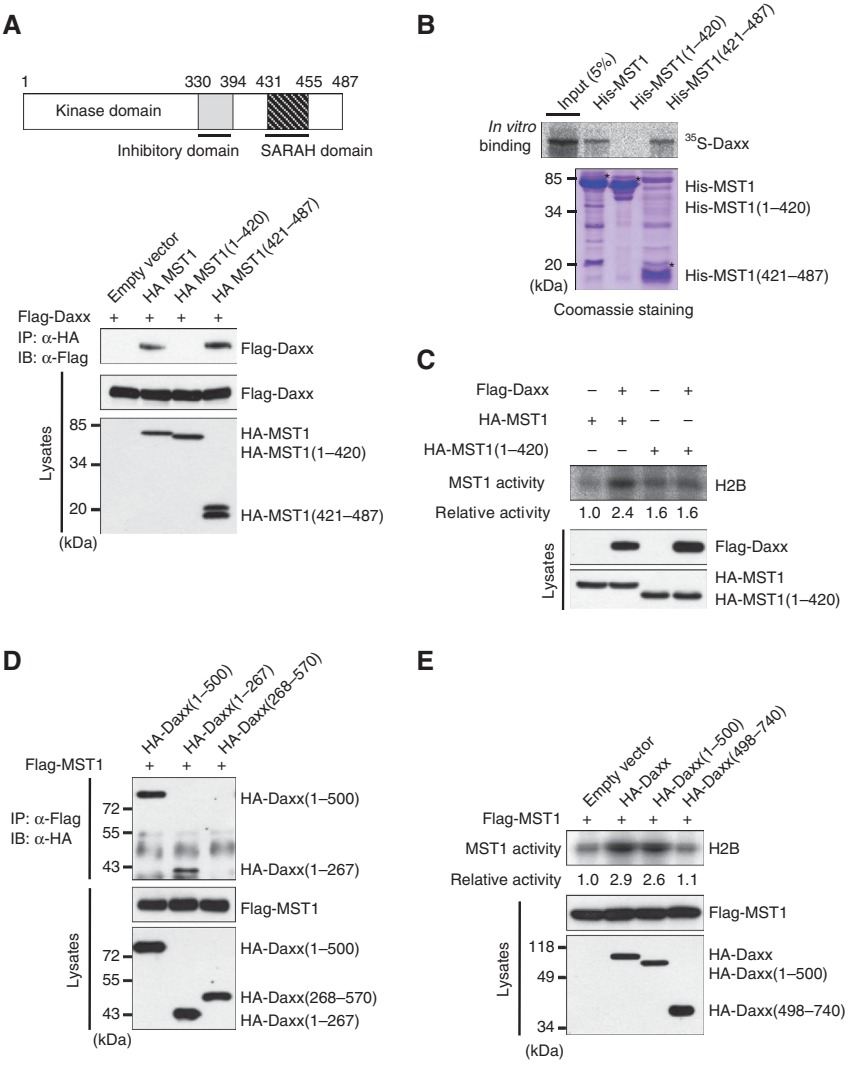

Figure 3 Characterization of the binding regions of MST1 and Daxx. (**A**) Schematic representation of the domain organization of human MST1 is shown in the upper panel. 293T cells were transfected for 48 h with a vector encoding Flag-Daxx together with vectors for HA-tagged MST1 variants, as indicated. Cell lysates were subjected to immunoprecipitation with anti-HA antibody, and the resulting precipitates were examined by immunoblot analysis with anti-Flag antibody. Cell lysates were also examined directly by immunoblot analysis with antibodies to Flag or to HA. (**B**) *In vitro* binding of Daxx to MST1 variants. *In vitro* translated ^{35}S-labelled Daxx was incubated for 3 h at 4°C with hexahistidine-tagged MST1 variants (full-length (1–420), (421–487)). The binding mixture was applied to Ni-NTA beads (Qiagen). Bead-bound ^{35}S-labelled proteins were eluted from the beads, subjected to SDS–PAGE, and analysed with Fuji BAS 2500. The polyacrylamide gel was also stained with Coomassie brilliant blue. Input, a portion (5%) of the ^{35}S-labelled protein input to the binding reaction. (**C**) 293T cells were transfected for 48 h with a vector for Flag-Daxx and a vector for either HA-MST1 or HA-MST1 (1–420), as indicated. Cell lysates were subjected to immunoprecipitation with anti-HA antibody and the resulting precipitates were examined for MST1 activity by immune complex kinase assay with histone H2B as substrate. (**D**) 293T cells were transfected for 48 h with a vector encoding Flag-MST1 together with vectors for HA-tagged Daxx variants, as indicated. Cell lysates were subjected to immunoprecipitation with anti-Flag antibody, and the resulting precipitates were examined by immunoblot analysis with anti-HA antibody. (**E**) 293T cells were transfected for 48 h with a vector for Flag-MST1 together with vectors for HA-tagged Daxx variants, as indicated. Cell lysates were subjected to immunoprecipitation and the resulting precipitates were examined for MST1 activity by immune complex kinase assay. Cell lysates were also examined directly by immunoblot analysis with antibodies to Flag or to HA.

binding data, ectopically expressed Daxx or Daxx (1–500) increased MST1 activity whereas Daxx (498–740) did not (Figure 3E).

Homodimerization of MST1 contributes to the mechanism of MST1 activation (Creasy *et al*, 1996; Glantschnig *et al*, 2002). Given that Daxx binds to MST1 (421–487) that includes the SARAH domain, which mediates MST1 homodimerization (Creasy *et al*, 1996; Scheel and Hofmann, 2003), we examined whether Daxx might regulate the homodimerization of MST1. We thus transfected Daxx$^{-/-}$ mouse embryonic fibroblasts (MEFs) with plasmids encoding Daxx, Flag-MST1, and HA-MST1, and subjected the cells to co-immunoprecipitation analysis. Flag-MST1 was associated with HA-MST1 only in the Daxx$^{-/-}$ MEF cells reconstituted with Daxx (Figure 4A). In comparison, Flag-MST1 did not form a complex with HA-MST1 (1–420) even in the cells reconstituted with Daxx (Figure 4B). Together, these results suggested that Daxx is indispensable for MST1 homodimerization, and that the SARAH domain of MST1 is required for the Daxx-dependent homodimerization of MST1.

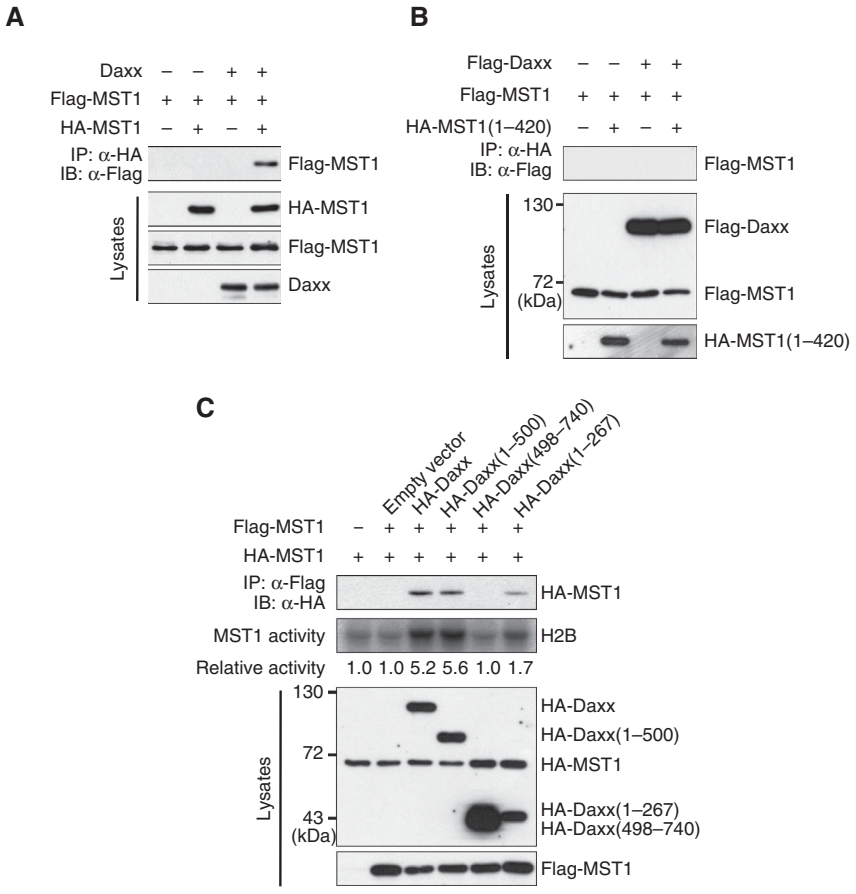

Figure 4 Daxx promotes the homodimerization of MST1. (**A**, **B**) Effect of ectopic Daxx on MST1 homodimerization in Daxx$^{-/-}$ MEFs. MEFs from Daxx-null mice were transfected for 48 h with the indicated combinations of plasmids encoding Flag-MST1, HA-MST1, and Daxx (**A**) or Flag-MST1, HA-MST (1–420), and Flag-Daxx (**B**). Cell lysates were subjected to immunoprecipitation with anti-HA antibody, and the resulting precipitates were subjected to immunoblot analysis with anti-Flag antibody. Cell lysates were also examined directly by immunoblotting with antibodies to Flag, to HA, or to Daxx. (**C**) Daxx$^{-/-}$ MEFs were transfected for 48 h with vectors encoding Flag-MST1, HA-MST1, and HA-tagged Daxx variants, as indicated. Cell lysates were subjected to immunoprecipitation with anti-Flag antibody, and the resulting precipitates were subjected to immunoblot analysis with anti-HA antibody as well as to an immune complex kinase assay for MST1 activity. Cell lysates were also examined directly by immunoblotting with antibodies to HA or to Flag.

We next examined the effects of Daxx and its various fragments on the homodimerization and kinase activity of MST1 in Daxx$^{-/-}$ MEFs by transfection experiments. MST1 homodimerization was detected in Daxx$^{-/-}$ MEFs reconstituted with Daxx, Daxx (1–500), or Daxx (1–267), but not in those expressing Daxx (498–740) (Figure 4C). The extent of MST1 homodimerization was smaller in Daxx$^{-/-}$ MEFs expressing Daxx (1–267) than in those expressing Daxx or Daxx (1–500). The kinase activity of Flag-MST1 was markedly increased in the Daxx$^{-/-}$ cells reconstituted with Daxx or Daxx (1–500), but not in those expressing Daxx (498–740). Daxx (1–267) also increased the kinase activity of Flag-MST1 in the transfected cells, but this effect was not as pronounced as that of Daxx or Daxx (1–500). Together, these results implicated MST1 homodimerization in the mechanism by which Daxx activates MST1. WW45 and Rassf proteins have been shown to interact with MST1 and thereby to regulate MST1-mediated signalling (Khokhlatchev *et al*, 2002; Callus *et al*, 2006; Oh *et al*, 2006; Lee *et al*, 2008). However, ablation of the WW45 or Rassf1 genes did not affect the Daxx-induced activation of MST1 in MEFs (Supplementary Figure S6), suggesting that neither WW45 nor Rassf1 is involved in the Daxx-mediated activation of MST1. It is also noteworthy that RNAi-mediated depletion of Rassf5 did not affect IFN-γ-induced MST1 activation in BV-2 cells (Supplementary Figure S7). Daxx has been found to interact with the promyelocytic leukaemia protein PML (Ishov *et al*, 1999; Zhong *et al*, 2000). Indeed, our co-immunoprecipitation data revealed that PML associated with Daxx in BV-2 cells (Supplementary Figure S8A). Noticeably, IFN-γ treatment increased the abundance of PML as well as Daxx in the cells, thereby enhancing the binding between Daxx and PML. However, PML did not associate with MST1 in the cells regardless of IFN-γ treatment. Immunoblot analysis with phospho-MST1 antibody also indicated that RNAi-mediated knockdown of PML did not affect the IFN-γ-induced activation of MST1 in BV-2 cells (Supplementary Figure S8B).

Daxx has also been shown to form homodimers (Song and Lee, 2003). Indeed, we detected the homodimerization of either Daxx or Daxx (1–500) by co-immunoprecipitation analysis with Daxx$^{-/-}$ MEFs (Figure 5A). In contrast, Daxx (1–267) (Figure 5A) or Daxx (498–740) (Supplementary Figure S9) did not appear to undergo homodimerization. These observations are consistent with the idea that the homodimerization of Daxx is crucial for its promotion of the homodimerization and activation of MST1. We further

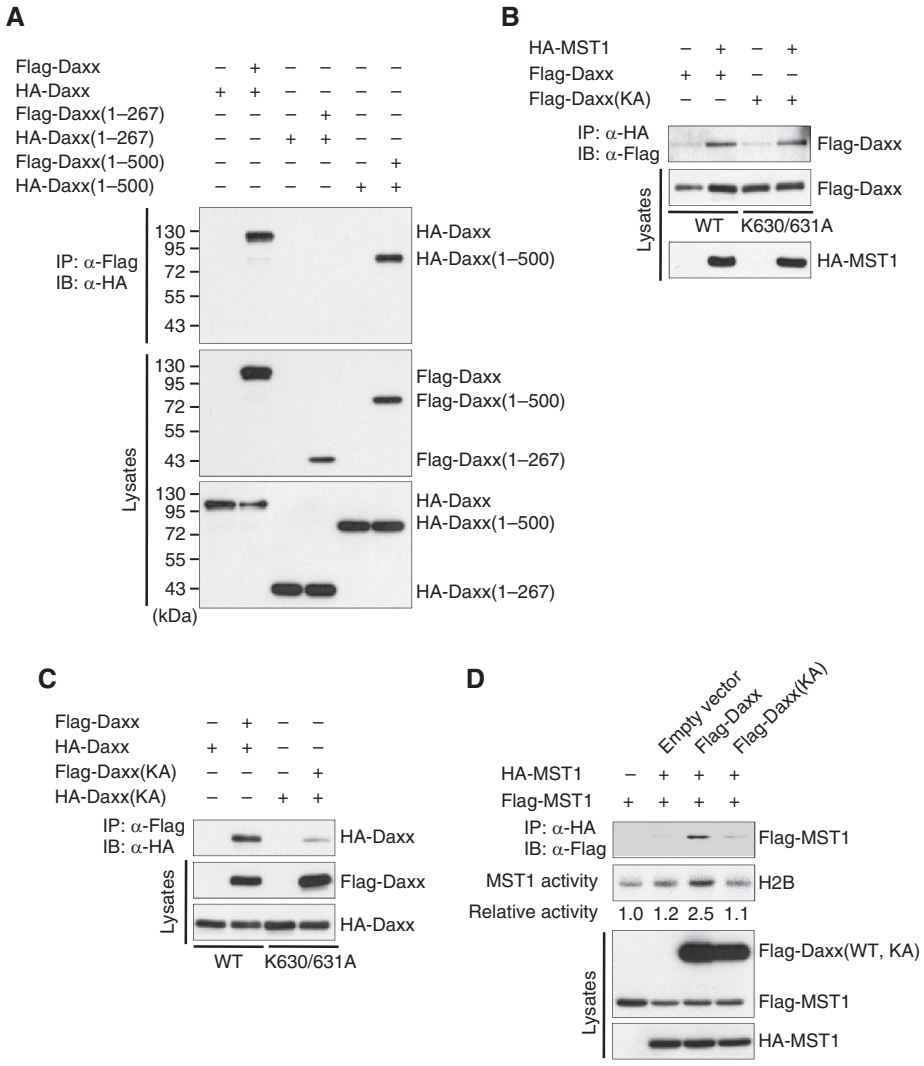

Figure 5 Effect of Daxx dimerization on the homodimerization and activation of MST1. (**A**) Daxx$^{-/-}$ MEFs were transfected for 48 h with the indicated combinations of plasmids for Flag- or HA-tagged Daxx variants, after which cell lysates were subjected to immunoprecipitation with anti-Flag antibody and the resulting precipitates were subjected to immunoblotting with anti-HA antibody. Cell lysates were also examined directly by immunoblot analysis with antibodies to Flag or to HA. (**B**) Daxx$^{-/-}$ MEFs were transfected with vectors for either Flag-Daxx or Flag-Daxx (K630/631A) alone or together with a vector for HA-MST1. Cell lysates were subjected to immunoprecipitation with anti-HA antibody, and the precipitates were examined by immunoblotting with anti-Flag antibody. Cell lysates were also examined directly by immunoblot analysis with antibodies to Flag or to HA. (**C**) Daxx$^{-/-}$ MEFs were transfected with vectors for Flag- or HA-tagged Daxx or Daxx (K630/631A). Cell lysates were subjected to immunoprecipitation with anti-Flag antibody, and the precipitates were examined by immunoblot analysis with anti-HA antibody. (**D**) Daxx$^{-/-}$ MEFs were transfected with vectors for Flag- or HA-tagged MST1 together with a vector for either Flag-Daxx or Flag-Daxx (K630/631A), as indicated, after which cell lysates were subjected to immunoprecipitation with anti-HA antibody. The resulting precipitates were subjected both to immunoblot analysis with anti-Flag antibody as well as to an immune complex kinase assay for MST1 activity.

tested this possibility with the use of the mutant Daxx (K630/631A), in which both Lys^{630} and Lys^{631} are replaced by alanine. Daxx (K630/631A) bound to MST1, as did wild-type Daxx (Figure 5B), but the mutant protein did not form homodimers efficiently (Figure 5C). We then compared the effects of Daxx and Daxx (K630/631A) on the homodimerization and kinase activity of MST1 in Daxx$^{-/-}$ MEFs transfected with the appropriate vectors. In contrast to the effects of Daxx, Daxx (K630/631A) did not induce the homodimerization or activation of MST1 (Figure 5D).

Daxx promotes the nuclear translocation of MST1

MST1, which contains two nuclear export signal (NES) consensus sequences near the COOH-terminus, is localized in the cytoplasm of resting cells as a result of its NES-dependent nuclear exclusion (Ura *et al*, 2001a). Given that Daxx resides primarily in the nucleus (Ishov *et al*, 1999), we examined whether Daxx might affect the subcellular localization of MST1 after transfecting COS-7 cells with vectors for Flag-MST1 and various HA-tagged Daxx variants. Confocal microscopy revealed that full-length Daxx, Daxx (1–500), and Daxx (498–740) were present in the nucleus, whereas Daxx (K630/631A) was present mostly in the cytoplasm (Figure 6A). The cytoplasmic localization of MST1 was not changed in the cells expressing Daxx (K630/631A) or Daxx (498–740). In contrast, MST1 was colocalized with Daxx or Daxx (1–500) in the nucleus. These results suggested that the nuclear localization and MST1-binding ability of Daxx are required for its

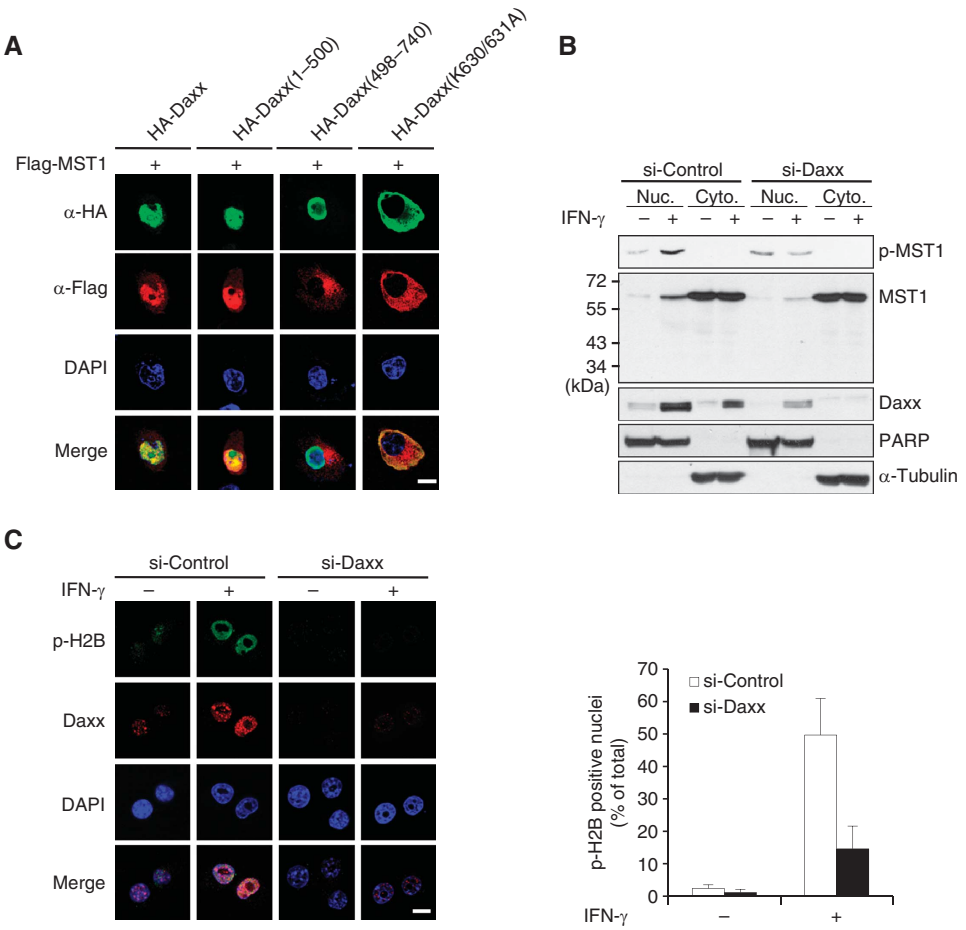

Figure 6 Daxx promotes the nuclear localization and activation of MST1. (**A**) COS-7 cells were transfected for 24 h with a vector for Flag-MST1 together with vectors for the indicated HA-tagged Daxx variants. The transfected cells were fixed, permeabilized, stained with DAPI, and subjected to immunostaining with antibodies to Flag or to HA. Images were acquired by confocal microscopy (Carl Zeiss, LSM 510 META). Scale bar, 10 μm. (**B**) BV-2/si-Control and BV-2/si-Daxx cells were incubated in the absence or presence of IFN-γ (100 U/ml) for 16 h, after which cell lysates were prepared and separated into the nuclear (Nuc.) and cytosolic (Cyto.) fractions. Each fraction was subjected to immunoblot analysis with antibodies to Thr^{183}-phosphorylated MST1 (p-MST1), to MST1, to Daxx, to poly(ADP-ribose) polymerase (PARP, nuclear marker), or to α-tubulin (cytosolic marker). (**C**) BV-2/si-Control and BV-2/si-Daxx cells were untreated or treated with IFN-γ (100 U/ml) for 16 h, fixed, permeabilized, stained with DAPI, and subjected to immunostaining with antibodies to Ser^{14}-phosphorylated histone H2B or to Daxx. The numbers of nuclei with the phosphorylated form of histone H2B were counted in randomly chosen fields in a confocal microscope (Carl Zeiss, LSM 510 META), and expressed as the percentages relative to total numbers of nuclei. At least 300 cells were scored for each treatment. Scale bar, 10 μm.

promotion of the nuclear translocation of MST1 from the cytoplasm.

Given that Daxx induced the nuclear translocation of MST1 in COS-7 cells, we examined whether the activation of MST1 by the IFN-γ-Daxx signalling pathway might be detected in the nucleus of microglial cells. IFN-γ induced an increase in the amount of MST1 in the nucleus in BV-2 cells expressing control siRNA but not in those expressing Daxx siRNA (Figure 6B). Moreover, immunoblot analysis with antibodies specific for MST1 phosphorylated on Thr^{183} (the active form of MST1) revealed that IFN-γ induced the activation of MST1 present in the nucleus, but not of that in the cytosol, in the cells expressing control siRNA. This effect of IFN-γ was abolished in the cells expressing Daxx siRNA. Furthermore, IFN-γ induced an increase in the phosphorylated form of histone H2B in the nucleus in BV-2 cells (Figure 6C). These effects of IFN-γ were not apparent in the cells expressing Daxx siRNA. These results thus suggested that IFN-γ-induced upregulation of Daxx expression promotes the MST1-mediated phosphorylation of histone H2B in the nucleus of microglial cells.

Daxx and MST1 mediate IFN-γ-induced apoptosis in microglia

Given that MST1 functions in IFN-γ-induced apoptosis and that Daxx mediates IFN-γ-induced MST1 activation in microglial cells, we examined whether Daxx-dependent MST1 activation contributes to IFN-γ-induced apoptosis in microglia. IFN-γ induced a marked increase in the incidence of apoptosis in primary rat microglia (Figure 7A) and BV-2 cells transfected with control GFP siRNA (Figure 7B), but this effect was suppressed by RNAi-mediated depletion of either Daxx (Figure 7A and B). As shown in Figures 1C and 2E, IFN-γ also induced the phosphorylation of histone H2B in rat primary microglia transfected with control siRNA, and again this effect was attenuated in cells transfected with either Daxx or MST1 siRNAs. Together, these results suggested that Daxx and MST1 mediate IFN-γ-induced apoptosis in microglia.

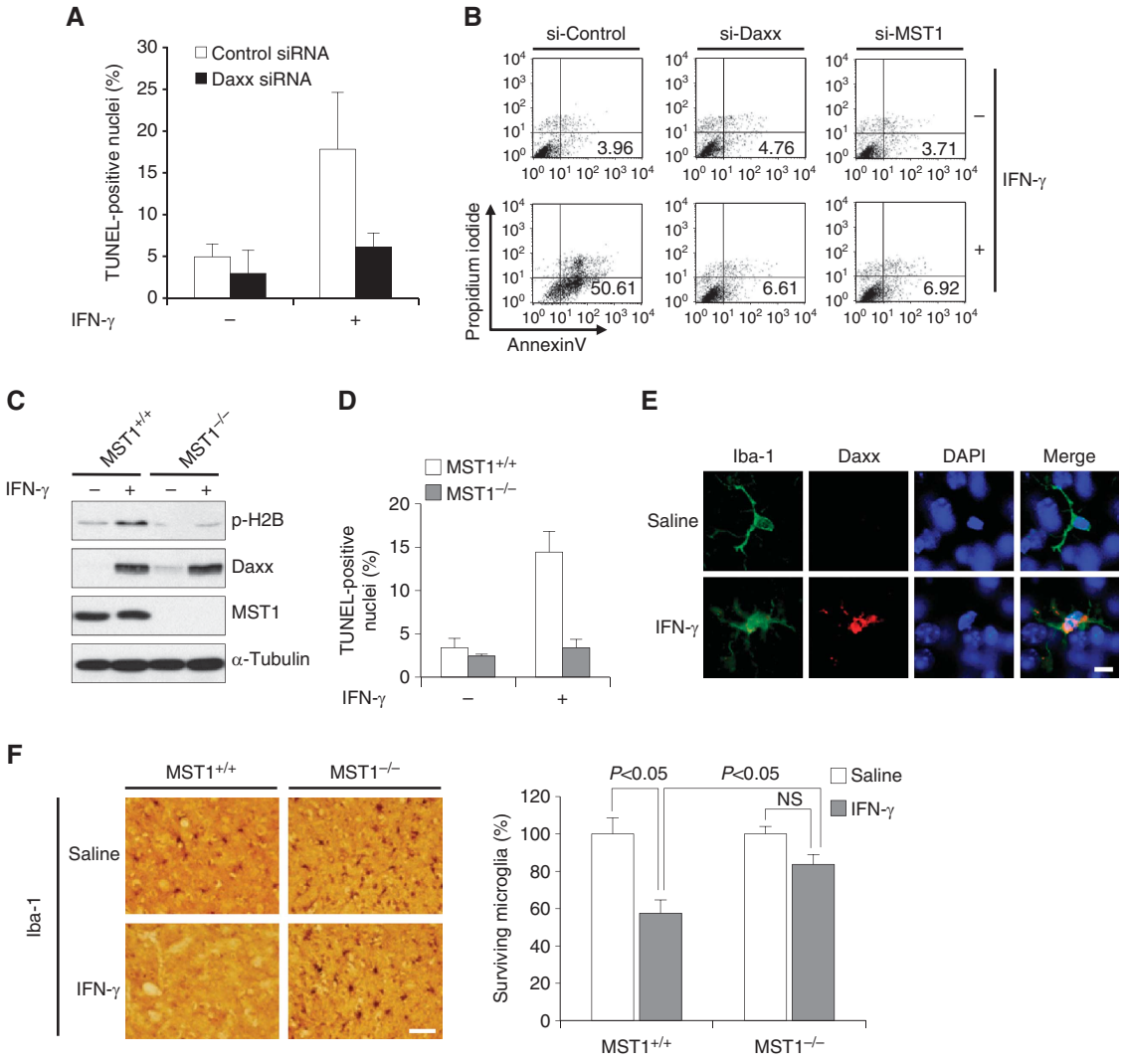

Figure 7 Ablation of Mst1 mitigates IFN-γ-induced microglial death. (**A**) Primary rat microglia were transfected for 24 h with siRNA oligonucleotides targeting GFP (control) or Daxx mRNAs and were then incubated for 48 h in the absence or presence of IFN-γ (100 U/ml). Apoptosis was analysed with TUNEL method. Data are the mean of triplicate determinations ± s.d. (**B**) BV-2/si-Control, BV-2/si-Daxx, and BV-2/si-MST1 cells were incubated in the absence or presence of IFN-γ (100 U/ml) for 48 h and were then stained with annexin V-FITC and propidium iodide for detection of apoptotic (annexin V-positive, propidium iodide-negative) cells by flow cytometry. Data are representative of three independent experiments. (**C**, **D**) Primary microglia isolated from wild-type (MST1 $^{+/+}$) or MST1-null mice were untreated or treated with IFN-γ (100 U/ml) for 16 h (**C**) or 48 h (**D**). (**C**) Cells were lysed and subjected to immunoblot analysis with antibodies to Ser^{14}-phosphorylated histone H2B (p-H2B), to Daxx, to MST1, or to α-tubulin. (**D**) Apoptotic cell death was analysed with TUNEL method. Data are the mean of triplicate determinations ± s.d. (**E**, **F**) WT mice alone (**E**) or WT and MST1-null mice (**F**) were subjected to stereotaxic injection of IFN-γ or PBS into the cerebral cortex. Brain sections adjacent to the injection sites were prepared at 1 day (**E**) or 2 days (**F**) after IFN-γ or PBS injection. (**E**) The sections were subjected to immunostaining with anti-Daxx and anti-Iba-1 antibodies followed by nuclear staining with DAPI. The images were visualized with Olympus BX51 fluorescence microscope equipped with Olympus DP70 digital camera. Scale bar, 10 μm. (**F**) The brain sections were subjected to immunohistochemical staining with anti-Iba-1 antibody (left panel). Iba-1-positive microglia in two regions adjacent to the injection sites were counted, and mean ± s.e.m. values for 10 regions from five animals are shown in the right panel. NS, not significant. Scale bar, 50 μm.

Finally, we examined the effects of IFN-γ on microglia of MST1 knockout mice. IFN-γ increased the abundance of Daxx in primary microglia from both wild-type and MST1$^{-/-}$ mice (Figure 7C). The MST1-deficient microglia, however, did not exhibit the IFN-γ-induced phosphorylation of histone H2B (Figure 7C) and apoptosis (Figure 7D) that were apparent in wild-type cells. Noticeably, IFN-γ did not induce expression of Daxx, MST1 activation, or apoptosis in astrocytes from wild-type mice (Supplementary Figure S10). IFN-γ-induced apoptosis in microglial cells from wild-type mice was not affected significantly by a pan-caspase inhibitor z-VAD-fmk (Supplementary Figure S10B).

We also investigated the effect of IFN-γ on the viability of microglia *in vivo*. Microglial induction of Daxx was observed in the brain of mice by immunohistochemistry 1 day after IFN-γ injection (Supplementary Figure S11). The induced Daxx was present mainly in the nucleus of microglia (Figure 7E). We then examined the viability of microglia in the brain of wild-type or MST1-null mice 2 days after IFN-γ injection. Immunohistochemical staining with antibody to the microglial marker Iba-1 revealed that IFN-γ induced a marked decrease in the number of microglia in the brain of wild-type mice (Figure 7F). In contrast, this effect of IFN-γ was not apparent in the brain of MST1-null mice.

In response to tissue injury or inflammatory stimuli, microglia become activated and subsequently produce both neurotrophic and neurotoxic substances (Streit *et al*, 1999; Liu and Hong, 2003). Persistent activation of microglia for extended periods of time may result in irreversible damage to neurons and contribute to the pathogenesis of neurological disorders (Block and Hong, 2005; Block *et al*, 2007; Rogers *et al*, 2007). It is therefore important that the promotion of inflammatory processes beneficial to tissue integrity by activated microglia be terminated in a timely manner, with one such means of termination being AICD. Our results now show that both Daxx and MST1 are key mediators of microglial cell death induced by the proinflammatory cytokine IFN-γ. Additionally, the MST1-mediated phosphorylation of histone H2B observed in IFN-γ-treated microglia implicates that this phosphorylation might be an integral part of the mechanism for the MST1-mediated cell death of microglia, given that MST1 promotes chromatin condensation associated with apoptosis by means of the Ser^{14} phosphorylation of histone H2B (Cheung *et al*, 2003). Aside from histone 2B, it is also equally possible that the components of the Hippo pathway may be involved in the mechanism of the MST1-mediated microglial cell death. NO is one of the players mediating AICD in microglia (Lee *et al*, 2001a, b; Mayo and Stein, 2007; Khazaei *et al*, 2008). Therefore, it is intriguing to understand the mechanistic link between MST1 and NO in IFN-γ-induced microglial cell death. In this regard, it is noticeable that siRNA-mediated depletion of MST1 did not affect the IFN-γ-induced NO production (Supplementary Figure S12), suggesting that MST1 signalling is not involved in IFN-γ-induced NO production in microglia. These data also implicate that NO may not be involved in the signalling events downstream of MST1 in IFN-γ-induced cell death in microglia. With these findings, one may propose that MST1 and NO mediate IFN-γ-induced microglial cell death through independent mechanisms. We do not rule out, however, another possibility that NO may act upstream of MST1 in the processes of IFN-γ-induced microglial cell death. Under certain conditions, MST1 has been reported to promote apoptotic events through the upregulation of the stress-induced protein kinases including JNK and p38 kinase (Graves *et al*, 1998; Ura *et al*, 2001b). However, either SP600125 (a JNK inhibitor) or SB203580 (a p38 inhibitor) did not inhibit IFN-γ-induced apoptosis in BV-2 cells (Supplementary Figure S13), suggesting that JNK or p38 kinase are not involved in the MST1-mediated apoptosis in microglia. Regardless of the upstream and downstream factors of MST1 responsible for IFN-γ-induced microglial cell death, our findings suggest that Daxx and MST1 may serve as new targets for the development of novel therapeutic agents for neurodegenerative disorders associated with neuroinflammation. It is also noteworthy that the IFN-γ-induced increases in Daxx expression as well as MST1 activation are also apparent in primary alveolar macrophages (Supplementary Figure S14).

The molecular mechanisms of MST1 regulation have remained largely unclear, with caspase-mediated cleavage having been the best characterized such mechanism (Graves *et al*, 2001; Cheung *et al*, 2003). Caspase-mediated cleavage of MST1 has been thought to liberate the NH_2-terminal kinase domain from the NES located in the regulatory COOH-terminal region, resulting in translocation of the kinase domain into the nucleus and consequent phosphorylation of nuclear substrates such as histone H2B (Ura *et al*, 2001a). It has been also thought that, if MST1 becomes activated by a cleavage-independent mechanism, the intact MST1 remains in the cytoplasm and phosphorylates its cytoplasmic substrates (Radu and Chernoff, 2009). This scenario is now challenged by our present data, indicating that Daxx induces both the nuclear translocation of intact MST1 and its activation in the nucleus. Our findings thus provide new insight into the regulation of MST1 and thus into how MST1 influences a variety of cellular events including cell proliferation and differentiation as well as apoptosis and morphogenesis.

Materials and methods

Antibodies and reagents

Rat monoclonal anti-HA antibody was obtained from Roche Applied Science, Mannheim, Germany. Mouse monoclonal antibodies to Flag and to α-tubulin as well as rabbit monoclonal antibody to HA were from Sigma (St Louis, MO). Rabbit polyclonal antibodies to MST1 and to Thr^{183}-phosphorylated MST1 were from Cell Signaling (Boston, MA), and rabbit monoclonal anti-histone H2B antibody was from Upstate Biotechnology (Lake Placid, NY). Mouse monoclonal and goat polyclonal antibodies to Daxx as well as rabbit polyclonal antibodies to Ser^{14}-phosphorylated histone H2B were obtained from Santa Cruz Biotechnology (Santa Cruz, CA). Rabbit polyclonal antibodies to Iba-1 were from Wako (Osaka, Japan), and OX-42 antibodies to CD11b were from Serotec (Oxford, UK). Murine and rat IFN-γ were purchased from PeproTech (Rocky Hill, NJ). Caspase inhibitor (z-VAD-fmk) and AG490 were from Calbiochem (San Diego, CA).

Cell culture and DNA transfection

Murine microglial BV-2, human embryonic kidney 293T, monkey kidney COS-7 cells, as well as MEFs (Ishov *et al*, 1999) derived from $Daxx^{-/-}$ mice were cultured under a humidified atmosphere of 5% CO_2 at 37°C in DMEM supplemented with 10% FBS. For primary culture of rat microglia, single cells were prepared from the cerebral cortex of 1-day-old Sprague-Dawley rats (Orient, Seoul, Korea) by trituation in minimal essential medium (GIBCO) supplemented with 10% FBS and 2 mM glutamine. The cells were plated in 75 cm^2 T-Flasks (SPL Life Sciences, Seoul, Korea) and incubated for 14 days, after which the flasks were gently shaken and the cells were isolated by filtration through a cell strainer with a pore size of 70 μm (Falcon). The cells were then plated in 60 mm culture dishes (1×10^5 cells/dish) for experiments. The quality of primary microglia was checked with immunostaining with antibody to the microglial marker Iba-1. More than 95% of the cells in primary cultures were Iba-1-positive cells. For DNA transfection, BV-2, 293T, and MEF cells were plated in 100 mm dishes at 1×10^6 cells/dish, grown for 48 h, and transfected with appropriate vectors with the use of Lipofectamine 2000 (Invitrogen). Primary rat microglial cells were transfected with indicated siRNA oligonucleotides with Hiperfect (Qiagen).

Plasmids

The pME18S vector containing cDNA for Flag-tagged MST1 was kindly provided by S Yonehara (Kyoto University, Japan). The pET-23b/MST1 (K59R) vector was described previously (Oh *et al*, 2006). To generate a plasmid encoding MST1 with an NH2-terminal HA tag, we subcloned MST1 cDNA into the pHM6 vector (Roche) with the use of PCR. The pRK5/Flag-Daxx, pET-28a/Daxx, pcDNA3/HA-Daxx, and pcDNA3 vectors encoding various deletion mutants of Daxx were kindly provided by S Kim (Seoul National University, Korea).

Immune complex kinase assay

Cells were lysed in a lysis buffer (Ryoo *et al*, 2004), and assayed for MST1 activity by immune complex kinase assay with histone H2B

as substrate, as previously described (Park *et al*, 2001; Ryoo *et al*, 2004).

Co-immunoprecipitation analysis

Co-immunoprecipitation was performed as described previously (Cho *et al*, 2003). In brief, cell lysates were centrifuged at 12 000 *g* for 20 min at 4°C, and the resulting supernatants were incubated at 4°C first for 2 h with the indicated antibodies and then for 1 h in the presence of protein G-conjugated Sepharose beads (Amersham Bioscience). The immunoprecipitates were subjected to immunoblot analysis with the indicated primary antibodies, and immunoreactive bands were visualized with horseradish peroxidase-conjugated secondary antibodies (Amersham Bioscience) and enhanced chemiluminescence reagents (Pierce).

In vitro binding assay

Full-length and deletion mutants of Daxx were translated *in vitro* in the presence of [^{35}S]methionine with the use of a Quick Coupled TnT kit (Promega). The ^{35}S-labelled proteins were incubated for 2 h at 4°C with bacterially expressed hexahistidine-tagged MST1 in a binding buffer (Cho *et al*, 2003), after which Ni-NTA beads (Qiagen) were added to the reaction mixture. Bead-bound proteins were washed three times with a washing buffer (50 mM Hepes, pH 7.5, 150 mM NaCl, 1 mM EDTA, 1 mM dithiothreitol, and 0.1% Tween 20), and eluted from the beads with a solution containing 50 mM sodium phosphate buffer (pH 8.0), 300 mM NaCl, and 250 mM imidazole. Eluted ^{35}S-labelled proteins were detected by SDS–PAGE and a Fuji BAS 2500 phosphoimager.

RNAi

The target sequences for MST1 or Daxx siRNAs were selected with the use of the siRNA target finder program of Ambion (http://www.ambion.com). They included 5′-AATCGGACCTGCAGGAGA TAA-3′ for mouse MST1 siRNA as well as 5′-AACAGGCGCATTGAA CGGCTC-3′ for mouse Daxx siRNAs. BV-2 cells were transfected with pSuper-retro (Oligoengine) vectors for mouse Daxx or MST1 siRNAs or with a control vector for GFP siRNA with the use of Lipofactamine, and stable transfectants were selected with the use of puromycin (3 μg/ml). Heterogeneous populations of the stable transfectants were used to avoid clonal variation. The siRNA duplexes specific for rat MST1 and Daxx mRNAs were synthesized chemically by Invitrogen and targeted to the sequences 5′-AATCGGACCTGCAGGAGATAA-3′ and 5′-AAGATGAAGCAGCTGC TCAGC-3′ (Lin *et al*, 2004), respectively; the GFP control siRNA was targeted to the sequences 5′-GTGCAAGTGCAAACCAGACTT-3′. Primary rat microglia were transfected with the siRNA duplexes with the use of Hiperfect (Qiagen).

Preparation of the nuclear and cytosolic fractions

BV-2 cells were trypsinized, washed with cold PBS twice, and suspended in buffer A (10 mM Hepes, pH 7.9, 0.1 mM EDTA, 0.1 mM EGTA, 10 mM KCl, 1 mM dithiothreitol, and 0.5 mM phenylmethylsulfonyl fluoride). After swelling on ice for 10 min, cells were solubilized by 0.1% Nonidet P-40 in buffer A and were then subjected to microcentrifugation at 6000 r.p.m. for 45 s. The supernatant (cytosolic fraction) was separated from the pellets. The pellets were subsequently washed twice with cold buffer B (0.32 M sucrose, 3 mM $CaCl_2$, 2 mM magnesium acetate, 0.1 mM EDTA, 10 mM Tris–HCl, pH 8.0, 1 mM dithiothreitol, and 0.5 mM phenylmethylsulfonyl fluoride) and centrifuged at 12 000 *g* at 4°C for 1 min. The resulting pellets were resuspended in cold buffer C (20 mM Hepes, pH 7.9, 1 mM EDTA, 1 mM EGTA, 400 mM NaCl, 1 mM dithiothreitol, and 1 mM phenylmethylsulfonyl fluoride), with vortexing every 10 min for a total of 40 min, and then centrifuged at 12 000 *g* at 4°C for 15 min. The supernatant (nuclear fraction) was separated from the insoluble parts.

Apoptosis assay

BV-2 cells were trypsinized, incubated with annexin V-FITC and propidium iodide (PI), and analysed by flow cytometry (FacsCalibur, Becton-Dickinson) with CellQuest software (BD Biosciences) for the detection of apoptotic cells (annexin V-positive, PI-negative). Primary rat microglia was incubated with TUNEL reaction mixture (Cho *et al*, 2003) for apoptosis analysis and then stained with DAPI. TUNEL-positive nuclei were analysed for apoptosis under Carl Zeiss Axiovert 200 fluorescence microscope. Data were expressed as the percentages of TUNEL-positive nuclei (the number of TUNEL-positive nuclei/the number of DAPI-stained nuclei $\times$ 100).

Yeast two-hybrid screening

Yeast two-hybrid screening was performed according to the manufacturer's protocol (Clontech). In brief, mouse MST1 (K59R) cDNA was inserted adjacent to the cDNA sequence for the DNA-binding domain of LexA in the pLexA bait vector. About 2×10^6 clones of a HeLa cDNA library (Clontech) were screened in *Saccharomyces cerevisiae* EGY48[p8op-lacZ]. Positive colonies were selected in the presence of X-gal in medium without adenine, uracil, tryptophan, and histidine, and the corresponding cDNAs were rescued from yeast by PCR with primers Bco I (5′-CCAGCTCTTGCT GAGTGGAGATG-3′) and Bco II (5′-GACAAGCCGACAACCTTGATTG GAG-3′). The DNA sequences of the resulting PCR products were determined with the use of the Bco I primer.

Stereotaxic injection in mouse brain

In vivo experiments with mice were performed in accordance with the approved protocols and guidelines of the Korea University Ethics Review Committee for animal experiments. IFN-γ (2000 U) or PBS was injected stereotaxically into the cerebral cortex of 8- to 12-week-old wild-type or MST1-null mice (Oh *et al*, 2009). The mice (body mass of ~30 g) were anaesthetized by intraperitoneal injection of a mixture of zoletil (75 mg/kg) and rompun (5 mg/kg) and were then positioned on a Kopf stereotaxic apparatus (model 900; David Kopf Instruments, Tujunga, CA). The stereotaxic coordinates for the cortex were anterior–posterior, +1.1 mm; medial–lateral, ±1.0 mm; and dorsal–ventral, −1.5 mm. The stereotaxic injection was performed at a rate of 0.2 μl/min, with the use of a microinjection autopump and a 10-μl Hamilton microsyringe filled with 1.5 μl of IFN-γ or PBS.

Immunohistochemistry

Mice were perfused transcardially with PBS and then with 3% paraformaldehyde. The brain was removed from the cranium, postfixed for 1 day, washed with PBS, and then immersed in 30% sucrose solution. The tissue was sectioned coronally at a thickness of 30 μm with a microtome, and every sixth serial section was selected and processed for immunostaining. The sections were fixed in 3% paraformaldehyde, washed with PBS, and incubated for 10 min in a solution containing 3% H_2O_2 and 0.25% Triton X-100 at room temperature, and then for 1 h with 10% horse serum. For microglia immunohistochemistry, the sections were incubated overnight at 4°C with rabbit antibodies to Iba-1 or to CD11b, for 2 h with biotin-conjugated goat antibodies to rabbit IgG, and for 1 h with avidin–biotin–peroxidase complex (Vector Laboratories). The sections were finally exposed to 3,3′-diaminobenzidine tetrahydrochloride dehydrate (Sigma), mounted on gelatin-coated slides, and examined with a bright-field microscope (Olympus). For Daxx immunohistochemistry, the sections were immunostained with goat anti-Daxx and rabbit anti-Iba-1 antibodies, then with Alexa 546-conjugated anti-goat and Alexa 488-conjugated anti-rabbit secondary antibodies (Invitrogen), followed by nuclear staining with DAPI (5 μg/ml). The fluorescent images were visualized with Olympus BX51 microscope equipped with Olympus DP70 digital camera.

Statistical analysis

Data are presented as means ± s.d. or s.e.m. ANOVA and the Student–Newman–Keuls test were used for multiple comparisons. A P-value of <0.05 was considered statistically significant.

Supplementary data

Supplementary data are available at *The EMBO Journal* Online (http://www.embojournal.org).

Acknowledgements

We thank V Bocchini, S Yonehara, and S Kim for providing BV-2 cells as well as MST1 or Daxx cDNA clones, respectively. This work was supported by the National Research Foundation Grant (2006-0093855), by Basic Science Research Program (2009-0080985) through the National Research Foundation of Korea (NRF), and a NRF Grant (20090081488) (E-JC), and the Creative Research Initiative Program (D-SL), and by the Korea Student Aid

Foundation (KOSAF) Grant (No. S2-2009-000-00791-1) (HJY) funded by the Ministry of Education, Science and Technology, South Korea.

Author contributions: HJY, JHY, JKL, KTN, KWY, SPO, HJO, JSC, and SGH performed the experiments and analysed the data. EHK constructed cytoplasmic Daxx mutant cDNAs. GGM provided Daxx-deficient MEFs. DSL and EJC directed the research. HJY and EJC designed the experiments and wrote the paper with input from GGM.

Conflict of interest

The authors declare that they have no conflict of interest.

References

Block ML, Hong JS (2005) Microglia and inflammation-mediated neurodegeneration: multiple triggers with a common mechanism. *Prog Neurobiol* **76:** 77–98

Block ML, Zecca L, Hong JS (2007) Microglia-mediated neurotoxicity: uncovering the molecular mechanisms. *Nat Rev Neurosci* **8:** 57–69

Callus BA, Verhagen AM, Vaux DL (2006) Association of mammalian sterile twenty kinases, Mst1 and Mst2, with hSalvador via C-terminal coiled-coil domains, leads to its stabilization and phosphorylation. *FEBS J* **273:** 4264–4276

Chan EH, Nousiainen M, Chalamalasetty RB, Schafer A, Nigg EA, Sillje HH (2005) The Ste20-like kinase Mst2 activates the human large tumor suppressor kinase Lats1. *Oncogene* **24:** 2076–2086

Cheung WL, Ajiro K, Samejima K, Kloc M, Cheung P, Mizzen CA, Beeser A, Etkin LD, Chernoff J, Earnshaw WC, Allis CD (2003) Apoptotic phosphorylation of histone H2B is mediated by mammalian sterile twenty kinase. *Cell* **113:** 507–517

Cho SG, Kim JW, Lee YH, Hwang HS, Kim MS, Ryoo K, Kim MJ, Noh KT, Kim EK, Cho JH, Yoon KW, Cho EG, Park HS, Chi SW, Lee MJ, Kang SS, Ichijo H, Choi EJ (2003) Identification of a novel antiapoptotic protein that antagonizes ASK1 and CAD activities. *J Cell Biol* **163:** 71–81

Creasy CL, Ambrose DM, Chernoff J (1996) The Ste20-like protein kinase, Mst1, dimerizes and contains an inhibitory domain. *J Biol Chem* **271:** 21049–21053

Dan I, Watanabe NM, Kusumi A (2001) The Ste20 group kinases as regulators of MAP kinase cascades. *Trends Cell Biol* **11:** 220–230

de Souza PM, Lindsay MA (2004) Mammalian Sterile20-like kinase 1 and the regulation of apoptosis. *Biochem Soc Trans* **32:** 485–488

Dong J, Feldmann G, Huang J, Wu S, Zhang N, Comerford SA, Gayyed MF, Anders RA, Maitra A, Pan D (2007) Elucidation of a universal size-control mechanism in Drosophila and mammals. *Cell* **130:** 1120–1133

Glantschnig H, Rodan GA, Reszka AA (2002) Mapping of MST1 kinase sites of phosphorylation. Activation and autophosphorylation. *J Biol Chem* **277:** 42987–42996

Graves JD, Draves KE, Gotoh Y, Krebs EG, Clark EA (2001) Both phosphorylation and caspase-mediated cleavage contribute to regulation of the Ste20-like protein kinase Mst1 during CD95/Fas-induced apoptosis. *J Biol Chem* **276:** 14909–14915

Graves JD, Gotoh Y, Draves KE, Ambrose D, Han DK, Wright M, Chernoff J, Clark EA, Krebs EG (1998) Caspase-mediated activation and induction of apoptosis by the mammalian Ste20-like kinase Mst1. *EMBO J* **17:** 2224–2234

Hanisch UK, Kettenmann H (2007) Microglia: active sensor and versatile effector cells in the normal and pathologic brain. *Nat Neurosci* **10:** 1387–1394

Hao Y, Chun A, Cheung K, Rashidi B, Yang X (2008) Tumor suppressor LATS1 is a negative regulator of oncogene YAP. *J Biol Chem* **283:** 5496–5509

Huang J, Wu S, Barrera J, Matthews K, Pan D (2005) The Hippo signaling pathway coordinately regulates cell proliferation and apoptosis by inactivating Yorkie, the Drosophila Homolog of YAP. *Cell* **122:** 421–434

Ishov AM, Sotnikov AG, Negorev D, Vladimirova OV, Neff N, Kamitani T, Yeh ET, Strauss III JF, Maul GG (1999) PML is critical for ND10 formation and recruits the PML-interacting protein daxx to this nuclear structure when modified by SUMO-1. *J Cell Biol* **147:** 221–234

Justice RW, Zilian O, Woods DF, Noll M, Bryant PJ (1995) The Drosophila tumor suppressor gene warts encodes a homolog of human myotonic dystrophy kinase and is required for the control of cell shape and proliferation. *Genes Dev* **9:** 534–546

Kennedy PS, Goyal RK, Hersh T (1972) Hereditary angioneurotic edema. A case with recurring abdominal pain. *Am J Dig Dis* **17:** 435–438

Khazaei MR, Habibi-Rezaei M, Karimzadeh F, Moosavi-Movahedi AA, Sarrafnejhad AA, Sabouni F, Bakhti M (2008) Microglial cell death induced by glycated bovine serum albumin: nitric oxide involvement. *J Biochem* **144:** 197–206

Khokhlatchev A, Rabizadeh S, Xavier R, Nedwidek M, Chen T, Zhang XF, Seed B, Avruch J (2002) Identification of a novel Ras-regulated proapoptotic pathway. *Curr Biol* **12:** 253–265

Lee J, Hur J, Lee P, Kim JY, Cho N, Kim SY, Kim H, Lee MS, Suk K (2001a) Dual role of inflammatory stimuli in activation-induced cell death of mouse microglial cells. Initiation of two separate apoptotic pathways via induction of interferon regulatory factor-1 and caspase-11. *J Biol Chem* **276:** 32956–32965

Lee JH, Kim TS, Yang TH, Koo BK, Oh SP, Lee KP, Oh HJ, Lee SH, Kong YY, Kim JM, Lim DS (2008) A crucial role of WW45 in developing epithelial tissues in the mouse. *EMBO J* **27:** 1231–1242

Lee P, Lee J, Kim S, Lee MS, Yagita H, Kim SY, Kim H, Suk K (2001b) NO as an autocrine mediator in the apoptosis of activated microglial cells: correlation between activation and apoptosis of microglial cells. *Brain Res* **892:** 380–385

Lehtinen MK, Yuan Z, Boag PR, Yang Y, Villen J, Becker EB, DiBacco S, de la Iglesia N, Gygi S, Blackwell TK, Bonni A (2006) A conserved MST-FOXO signaling pathway mediates oxidative-stress responses and extends life span. *Cell* **125:** 987–1001

Lin DY, Fang HI, Ma AH, Huang YS, Pu YS, Jenster G, Kung HJ, Shih HM (2004) Negative modulation of androgen receptor transcriptional activity by Daxx. *Mol Cell Biol* **24:** 10529–10541

Liu B, Hong JS (2003) Role of microglia in inflammation-mediated neurodegenerative diseases: mechanisms and strategies for therapeutic intervention. *J Pharmacol Exp Ther* **304:** 1–7

Liu B, Wang K, Gao HM, Mandavilli B, Wang JY, Hong JS (2001) Molecular consequences of activated microglia in the brain: overactivation induces apoptosis. *J Neurochem* **77:** 182–189

Mayo L, Jacob-Hirsch J, Amariglio N, Rechavi G, Moutin MJ, Lund FE, Stein R (2008) Dual role of CD38 in microglial activation and activation-induced cell death. *J Immunol* **181:** 92–103

Mayo L, Stein R (2007) Characterization of LPS and interferon-gamma triggered activation-induced cell death in N9 and primary microglial cells: induction of the mitochondrial gateway by nitric oxide. *Cell Death Differ* **14:** 183–186

Meydan N, Grunberger T, Dadi H, Shahar M, Arpaia E, Lapidot Z, Leeder JS, Freedman M, Cohen A, Gazit A, Levitzki A, Roifman CM (1996) Inhibition of acute lymphoblastic leukaemia by a Jak-2 inhibitor. *Nature* **379:** 645–648

Neumann H (2001) Control of glial immune function by neurons. *Glia* **36:** 191–199

Oh H, Irvine KD (2009) *In vivo* analysis of Yorkie phosphorylation sites. *Oncogene* **28:** 1916–1927

Oh HJ, Lee KK, Song SJ, Jin MS, Song MS, Lee JH, Im CR, Lee JO, Yonehara S, Lim DS (2006) Role of the tumor suppressor RASSF1A in Mst1-mediated apoptosis. *Cancer Res* **66:** 2562–2569

Oh S, Lee D, Kim T, Kim TS, Oh HJ, Hwang CY, Kong YY, Kwon KS, Lim DS (2009) Crucial role for Mst1 and Mst2 kinases in early embryonic development of the mouse. *Mol Cell Biol* **29:** 6309–6320

Park HS, Lee JS, Huh SH, Seo JS, Choi EJ (2001) Hsp72 functions as a natural inhibitory protein of c-Jun N-terminal kinase. *EMBO J* **20:** 446–456

Pocock JM, Kettenmann H (2007) Neurotransmitter receptors on microglia. *Trends Neurosci* **30:** 527–535

Praskova M, Xia F, Avruch J (2008) MOBKL1A/MOBKL1B phosphorylation by MST1 and MST2 inhibits cell proliferation. *Curr Biol* **18:** 311–321

Radu M, Chernoff J (2009) The DeMSTification of mammalian Ste20 kinases. *Curr Biol* **19:** R421–R425

Rogers J, Mastroeni D, Leonard B, Joyce J, Grover A (2007) Neuroinflammation in Alzheimer's disease and Parkinson's disease: are microglia pathogenic in either disorder? *Int Rev Neurobiol* **82:** 235–246

Ryoo K, Huh SH, Lee YH, Yoon KW, Cho SG, Choi EJ (2004) Negative regulation of MEKK1-induced signaling by glutathione S-transferase Mu. *J Biol Chem* **279:** 43589–43594

Scheel H, Hofmann K (2003) A novel interaction motif, SARAH, connects three classes of tumor suppressor. *Curr Biol* **13:** R899–R900

Song JJ, Lee YJ (2003) Role of the ASK1-SEK1-JNK1-HIPK1 signal in Daxx trafficking and ASK1 oligomerization. *J Biol Chem* **278:** 47245–47252

Strano S, Munarriz E, Rossi M, Castagnoli L, Shaul Y, Sacchi A, Oren M, Sudol M, Cesareni G, Blandino G (2001) Physical interaction with Yes-associated protein enhances p73 transcriptional activity. *J Biol Chem* **276:** 15164–15173

Streit WJ, Walter SA, Pennell NA (1999) Reactive microgliosis. *Prog Neurobiol* **57:** 563–581

Takeuchi H, Wang J, Kawanokuchi J, Mitsuma N, Mizuno T, Suzumura A (2006) Interferon-gamma induces microglial-activation-induced cell death: a hypothetical mechanism of relapse and remission in multiple sclerosis. *Neurobiol Dis* **22:** 33–39

Ura S, Masuyama N, Graves JD, Gotoh Y (2001a) Caspase cleavage of MST1 promotes nuclear translocation and chromatin condensation. *Proc Natl Acad Sci USA* **98:** 10148–10153

Ura S, Masuyama N, Graves JD, Gotoh Y (2001b) MST1-JNK promotes apoptosis via caspase-dependent and independent pathways. *Genes Cells* **6:** 519–530

Vichalkovski A, Gresko E, Cornils H, Hergovich A, Schmitz D, Hemmings BA (2008) NDR kinase is activated by RASSF1A/MST1 in response to Fas receptor stimulation and promotes apoptosis. *Curr Biol* **18:** 1889–1895

Xu T, Wang W, Zhang S, Stewart RA, Yu W (1995) Identifying tumor suppressors in genetic mosaics: the Drosophila lats gene encodes a putative protein kinase. *Development* **121:** 1053–1063

Yagi R, Chen LF, Shigesada K, Murakami Y, Ito Y (1999) A WW domain-containing yes-associated protein (YAP) is a novel transcriptional co-activator. *EMBO J* **18:** 2551–2562

Zhao B, Wei X, Li W, Udan RS, Yang Q, Kim J, Xie J, Ikenoue T, Yu J, Li L, Zheng P, Ye K, Chinnaiyan A, Halder G, Lai ZC, Guan KL (2007) Inactivation of YAP oncoprotein by the Hippo pathway is involved in cell contact inhibition and tissue growth control. *Genes Dev* **21:** 2747–2761

Zhong S, Salomoni P, Ronchetti S, Guo A, Ruggero D, Pandolfi PP (2000) Promyelocytic leukemia protein (PML) and Daxx participate in a novel nuclear pathway for apoptosis. *J Exp Med* **191:** 631–640

